

# Quantum thermal machines in BTZ black hole spacetime

Dimitris Moustos<sup>1,\*</sup> and Obinna Abah<sup>1,†</sup>

<sup>1</sup>*School of Mathematics, Statistics, and Physics, Newcastle University,  
Newcastle upon Tyne NE1 7RU, United Kingdom*

(Dated: March 19, 2025)

We investigate an Otto thermodynamic cycle with a qubit Unruh-DeWitt detector as the working medium, coupled to a massless, conformally coupled scalar quantum field in the Hartle-Hawking vacuum in a (2+1)-dimensional BTZ black hole spacetime. We employ the thermal properties of the field to model heat and cold reservoirs between which the thermal machine operates. Treating the detector as an open quantum system, we employ a master equation to study its finite-time dynamics during each cycle stroke. We evaluate the output performance of the Otto heat engine and refrigerator by computing, respectively, the total work output and the cooling power for each of the Neumann, transparent, and Dirichlet boundary condition cases satisfied by the field at spatial infinity. Furthermore, we evaluate the optimal performance of the thermal machine by analyzing its efficiency at maximum power output and ecological impact. Our study presents a general framework for understanding the finite-time operation of relativistic quantum thermal machines, focusing on their energy optimization.

## I. INTRODUCTION

The technological advances achieved in the past decade in the fabrication of miniaturized nanoscale devices, along with the rapid development of quantum thermodynamics [1–4], have paved the way for the design of novel thermal machines that operate in the quantum regime [5]. Among them, the quantum Otto cycle [6–8] – comprising two adiabatic and two isochoric processes – is the most widely studied because it allows an explicit identification of heat and work exchanges in each process step. When operating as a heat engine, the Otto machine converts absorbed heat from a hot reservoir to work, while as a refrigerator, it consumes work to extract heat from a cold reservoir.

The second law of thermodynamics imposes a universal upper bound on the efficiency of heat engines, given by the Carnot efficiency [9],  $\eta_C = (T_h - T_c)/T_h$ , where  $T_h$  and  $T_c$  are the temperatures of the hot and cold reservoirs respectively. Similarly, the maximum coefficient of performance (COP) for refrigerators is  $\varepsilon_C = T_c/(T_h - T_c)$  [9]. However, these Carnot bounds are only obtained in the limit of infinitely slow strokes. More relevant for real thermal machines that operate in finite time are the efficiency at maximum power (EMP) [10, 11],  $\eta^*$ , for heat engines, and the COP at maximum figure of merit [7],  $\varepsilon^*$ , for refrigerators.

In quantum field theory, the notions of a vacuum state and particle number become observer-dependent in curved spacetimes or for non-inertial observers [12]. This is exemplified by the Hawking [13] and Unruh [14] effects. The Unruh effect states that a uniformly accelerating observer perceives the Minkowski vacuum state of a quantum field as a thermal state, with a temperature proportional to their acceleration. Similarly, the Hawking

effect describes how an observer near a black hole horizon detects a thermal spectrum of particles—the Hawking radiation—emitted by the black hole due to quantum vacuum fluctuations. Hawking and Unruh effects reveal a close connection between quantum physics, relativity, and thermodynamics.

An operational way to probing the particle content of a quantum field is through the Unruh-DeWitt (UDW) detector [14–16], a pointlike two-level quantum system (qubit) that locally interacts with the field. Excitations of the detector are interpreted to result from the absorption of field quanta, i.e., particles. Initially introduced to probe the particle phenomenology in the Unruh and Hawking effects, nowadays the UDW detector model is widely employed in relativistic quantum information [17], having found many applications in implementing quantum information protocols in relativistic settings.

The thermal response of uniformly accelerated detectors has been recently used to introduce the concept of a Unruh quantum Otto heat engine [18–23], where the detector serves as the working medium, undergoing an Otto thermodynamic cycle. During the isochoric stages of the cycle, the detector maintains constant acceleration while interacting weakly with a quantum field, which, due to the Unruh effect, effectively behaves as a thermal reservoir. Thus, by adjusting the magnitude of acceleration, one can simulate hot and cold heat reservoirs, allowing the engine to extract useful work.

Later studies have expanded upon the concept of the Unruh Otto heat engine by introducing a more general model of a relativistic quantum Otto engine, which builds on the effective temperatures observed by detectors following stationary trajectories while interacting with quantum fields in Gaussian states in curved spacetime backgrounds [24]. In this setup, the work that can be extracted by a detector following a circular trajectory has been specifically investigated. Moreover, additional studies explore the effects of relativistic motion of detectors through thermal field baths [25, 26], as well as

\* [dimitris.moustos@newcastle.ac.uk](mailto:dimitris.moustos@newcastle.ac.uk)

† [obinna.abah@newcastle.ac.uk](mailto:obinna.abah@newcastle.ac.uk)

instantaneous detector-field interactions [26, 27], on the performance of the Otto engine and the amount of extracted work.

In this paper, we utilize the thermal response of a UDW detector to a quantum field in a black hole background, to model the field as a heat reservoir and introduce a quantum Otto thermodynamic cycle. In particular, during the isochoric strokes of the Otto cycle, the detector interacts with a massless, conformally coupled scalar quantum field in the Hartle-Hawking vacuum state in a (2+1)-dimensional Bañados-Teitelboim-Zanelli (BTZ) black hole spacetime [28, 29]. The Wightman two-point correlation function of the conformally coupled field in this case is analytically evaluated [30, 31], facilitating the investigation of the detector dynamics. This has been employed, for example, in studying transition rates [32–34], the response of a detector to a black hole in a superposition of masses [35], and the process of extracting correlations from the quantum field vacuum [36, 37]. Related studies have investigated the performance of quantum batteries—modeled as UDW detectors—in the BTZ spacetime [38], as well as the efficiency of a Brayton thermodynamic cycle using the BTZ black hole as a working medium [39].

We treat the UDW detector as an open quantum system, with the conformally coupled field playing the role of the environment, and describe its time evolution using a master equation of the Gorini–Kossakowski–Sudarshan–Lindblad (GKSL) form [40]. By employing a finite-time analysis of the detector’s dynamics, we explicitly investigate how the thermal machine’s performance depends on the Neumann, transparent, and Dirichlet boundary conditions satisfied by the field at spatial infinity. This analysis is not possible in the long-time asymptotic limit, where the detector’s reduced density matrix reaches a unique thermal equilibrium state, leading to identical behavior for all three boundary conditions.

In what follows, we consider the Otto thermal machine to operate either as a heat engine or as a refrigerator. In the first scenario, we evaluate the total work output of the engine, optimizing its performance by analyzing its EMP. When the machine functions as a refrigerator, we assess its cooling power and optimize its performance by studying the COP at the maximum figure of merit [7, 8]. Our analysis identifies the Neumann boundary condition as the optimal choice for finite-time operations of the machine. In the heat engine case, it yields the highest work output among the three boundary conditions, with an efficiency at maximum power that exceeds the Curzon-Ahlborn efficiency [10]. For the refrigerator case, it enables the absorption of the maximum amount of heat from the cold reservoir. Additionally, the Neumann boundary condition allows the detector to achieve thermalization with the hot and cold reservoirs at earlier times than the other two cases. In addition, we study the optimal performance of the Otto cycle in terms of the ecological criterion [41], which balances the trade-off

between high power output and low entropy production.

The paper is organized as follows. In Sec. II, we introduce the UDW particle detector model and then present its time evolution in the framework of open systems. In Sec. III, we investigate the dynamics of a detector interacting with a conformally coupled scalar field in the BTZ black hole spacetime, analyzing how it is affected by the different boundary conditions imposed on the quantized field. In Sec IV, we introduce a quantum Otto thermal machine in the BTZ spacetime, where the detector serves as the working medium, and evaluate its overall performance when operating as either a heat engine or a refrigerator. Finally, in Sec. V, we summarize and discuss our results. Throughout the paper we denote spatial vectors with boldface letters ( $\mathbf{x}$ ), while spacetime vectors are represented by sans-serif characters ( $x$ ). Unless otherwise specified we set  $\hbar = c = k_B = 1$ .

## II. THE UDW DETECTOR MODEL

We consider a Unruh-DeWitt detector [14–16], modeled as a pointlike two-level quantum system (qubit) having a ground state  $|g\rangle$  and an excited state  $|e\rangle$ , separated by an energy gap  $\Omega$ . The Hamiltonian that describes the qubit detector is

$$H_0 = \frac{\Omega}{2} \sigma_3, \quad (1)$$

where  $\sigma_3$  is the Pauli-Z matrix. The detector moves along a worldline  $x(\tau)$  parametrized by its proper time  $\tau$ , and is linearly coupled to a quantum field  $\Phi(x)$ . In the interaction picture, the Hamiltonian that describes the interaction between the detector and the field reads

$$H_{\text{int}}(\tau) = \lambda \mu(\tau) \Phi(x(\tau)), \quad (2)$$

where  $\lambda$  is a coupling constant,

$$\mu(\tau) = e^{i\Omega\tau} \sigma_+ + e^{-i\Omega\tau} \sigma_-, \quad (3)$$

is the detector’s monopole moment operator expressed in terms of the ladder operators  $\sigma_+ = |e\rangle \langle g|$  and  $\sigma_- = |g\rangle \langle e|$  of the Pauli algebra, and  $\Phi(x(\tau))$  is the field evaluated along the detector’s worldline. The interaction Hamiltonian, Eq. (2), represents a special case of the spin-boson model Hamiltonian [40]. This suggests the treatment of a UDW detector as an open quantum system, with the quantum field playing the role of the environment inducing dissipation, noise, and decoherence (see, e.g., [42–47]).

### A. Open system dynamics

Now, we consider that the quantum field is prepared in a state  $|\Psi\rangle$ , and introduce the Wightman two-point correlation function of the field,

$$\mathcal{W}(\tau, \tau') := \langle \Psi | \Phi(x(\tau)) \Phi(x(\tau')) | \Psi \rangle, \quad (4)$$

evaluated along the detector's worldline. The correlation function, Eq. (4), incorporates all the information related to the state of the field, the trajectory of the detector and the structure of the background spacetime. We next focus on detectors that follow stationary trajectories and fields that are prepared in stationary states. In these cases, the Wightman function, Eq. (4), depends only on the proper time difference  $\tau - \tau'$  between two points on the detectors' worldline, i.e.,  $\mathcal{W}(\tau, \tau') = \mathcal{W}(\tau - \tau')$  [12, 48].

We introduce the Laplace transform, at imaginary argument  $i\Omega$ , of stationary Wightman functions,

$$\widehat{\mathcal{W}}(\Omega) \equiv \int_0^\infty ds e^{-i\Omega s} \mathcal{W}(s) = \frac{\Gamma(\Omega)}{2} + iS(\Omega), \quad (5)$$

where it is decomposed into its real,  $\Gamma(\Omega) = 2\text{Re}[\widehat{\mathcal{W}}(\Omega)]$ , and imaginary,  $S(\Omega) = \text{Im}[\widehat{\mathcal{W}}(\Omega)]$ , parts respectively. Employing the symmetry  $\widehat{\mathcal{W}}(s) = \mathcal{W}(-s)$ , where the overline denotes complex conjugation, it can be shown that

$$\Gamma(\Omega) := \int_{-\infty}^{+\infty} ds e^{-i\Omega s} \mathcal{W}(s). \quad (6)$$

The above Fourier transform of the Wightman function defines the *transition rate* [12] of the detector, i.e., the detector's probability to transition between its energy levels per unit time, due to its interaction with the field.

We assume that initially the detector and the field are in an uncorrelated state,  $\rho_{\text{tot}}(0) = \rho(0) \otimes |\Psi\rangle\langle\Psi|$ . In the Born-Markov approximation, the Schrödinger picture evolution of the reduced density matrix of the detector is described by the second-order master equation [43, 44]:

$$\dot{\rho}(\tau) = -i[H_{\text{eff}}, \rho(\tau)] + \mathcal{D}(\rho(\tau)), \quad (7)$$

where the dissipator reads

$$\begin{aligned} \mathcal{D}(\rho(\tau)) = & \lambda^2 \Gamma(-\Omega) \left( \sigma_- \rho \sigma_+ - \frac{1}{2} \{ \sigma_+ \sigma_-, \rho \} \right) \\ & + \lambda^2 \Gamma(\Omega) \left( \sigma_+ \rho \sigma_- - \frac{1}{2} \{ \sigma_- \sigma_+, \rho \} \right), \end{aligned} \quad (8)$$

and the effective Hamiltonian is  $H_{\text{eff}} = \tilde{\Omega} \sigma_z / 2$ , where  $\tilde{\Omega} := \Omega + \lambda^2 (S(-\Omega) - S(\Omega))$  is the Lamb shifted frequency.

For a general density matrix of the detector

$$\rho(\tau) = \frac{1}{2} (I + \mathbf{r}(\tau) \cdot \boldsymbol{\sigma}), \quad (9)$$

where  $\mathbf{r}$  is the Bloch vector, we solve the master equation

(7) to obtain

$$\begin{aligned} r_1(\tau) &= e^{-\lambda^2 \frac{\tilde{\Omega}}{2} \tau} \left( r_1(0) \cosh(\tilde{\Omega} \tau) - r_2(0) \sinh(\tilde{\Omega} \tau) \right), \\ r_2(\tau) &= e^{-\lambda^2 \frac{\tilde{\Omega}}{2} \tau} \left( r_2(0) \cosh(\tilde{\Omega} \tau) - r_1(0) \sinh(\tilde{\Omega} \tau) \right), \\ r_3(\tau) &= e^{-\lambda^2 \gamma \tau} r_3(0) + \kappa \left( 1 - e^{-\lambda^2 \gamma \tau} \right), \end{aligned} \quad (10)$$

where we have defined the decay rate

$$\gamma := \Gamma(\Omega) + \Gamma(-\Omega), \quad (11)$$

and, for simplicity, the ratio

$$\kappa := \frac{\Gamma(\Omega) - \Gamma(-\Omega)}{\Gamma(\Omega) + \Gamma(-\Omega)}. \quad (12)$$

### III. UDW DETECTOR IN BTZ SPACETIME

Here, we consider a UDW detector interacting with a massless, conformally coupled scalar quantum field  $\varphi(\mathbf{x})$  in a (2+1)-dimensional BTZ black hole background [28, 29]. The (spinless) BTZ black hole is described by the metric,

$$ds^2 = -\frac{r^2 - r_H^2}{\ell^2} dt^2 + \frac{\ell^2}{r^2 - r_H^2} dr^2 + r^2 d\phi^2, \quad (13)$$

in Schwarzschild-like coordinates with  $t \in (-\infty, \infty)$ ,  $r \in (0, \infty)$ ,  $\phi \in [0, 2\pi)$ . The metric is a vacuum solution to the Einstein field equations with a negative cosmological constant,  $\Lambda = -1/\ell^2$ , where  $\ell$  is the anti-de Sitter length. It is asymptotic to anti-de Sitter (AdS) space and admits a horizon at  $r_H = \sqrt{M}\ell$ , where  $M$  represents the mass of the black hole.

The Wightman function  $\mathcal{W}_{\text{BTZ}}(\mathbf{x}, \mathbf{x}') = \langle 0 | \varphi(\mathbf{x}) \varphi(\mathbf{x}') | 0 \rangle$  for a conformally coupled scalar field in the vacuum state  $|0\rangle$  in the BTZ spacetime is obtained in terms of the corresponding vacuum two-point correlation function  $\mathcal{W}_{\text{AdS}}(\mathbf{x}, \mathbf{x}')$  in anti-de Sitter space by means of the method of images and is given by [30, 31]:

$$\begin{aligned} \mathcal{W}_{\text{BTZ}}(\mathbf{x}, \mathbf{x}') &= \sum_{n=-\infty}^{+\infty} \mathcal{W}_{\text{AdS}}(\mathbf{x}, Z^n \mathbf{x}') \\ &= \frac{1}{4\sqrt{2}\pi\ell} \sum_{n=-\infty}^{+\infty} \left( \frac{1}{\sqrt{\sigma(\mathbf{x}, Z^n \mathbf{x}')}} - \frac{\zeta}{\sqrt{\sigma(\mathbf{x}, Z^n \mathbf{x}') + 2}} \right) \end{aligned} \quad (14)$$

where  $Z$  is the action  $Z : (t, r, \phi) \mapsto (t, r, \phi + 2\pi)$ , the parameter  $\zeta \in \{-1, 0, 1\}$  specifies respectively the Neumann ( $\zeta = -1$ ), transparent ( $\zeta = 0$ ), and Dirichlet ( $\zeta = 1$ ) boundary conditions imposed on the field at spatial infinity, and

$$\sigma(x, Z^n x') = \frac{rr'}{r_H^2} \cosh\left(\frac{r_H}{\ell}(\Delta\phi - 2\pi n)\right) - 1 - \frac{\sqrt{(r^2 - r_H^2)(r'^2 - r_H^2)}}{r_H^2} \cosh\left(\frac{r_H}{\ell^2}\Delta t\right), \quad (15)$$

with  $\Delta\phi = \phi - \phi'$  and  $\Delta t = t - t'$ . Dirichlet and Neumann boundary conditions are imposed on the field to address the lack of global hyperbolicity in AdS spacetime (and consequently in BTZ spacetime), ensuring a well-defined quantization scheme. Alternatively, a quantization scheme can also be defined without imposing boundary conditions on AdS, known as the transparent boundary condition [49].

### A. Response of the detector

Then, we consider that the UDW detector is kept in a fixed position outside the black hole horizon, that is, following the worldline  $x(\tau) = ((-g_{00})^{-1/2}\tau, r, \phi)$ . The correlation function  $\mathcal{W}_{\text{BTZ}}(x, x')$  is shown [30, 31] to be periodic in imaginary time for each of the three boundary conditions, satisfying the Kubo-Martin-Schwinger (KMS) condition [50, 51],

$$\mathcal{W}_{\text{BTZ}}(\tau) = \mathcal{W}_{\text{BTZ}}(-\tau - i\beta), \quad (16)$$

in the exterior of the black hole, with a period  $\beta$  given by

$$\beta^{-1} = T = \frac{r_H}{2\pi\ell\sqrt{r^2 - r_H^2}}. \quad (17)$$

$T$  is interpreted as a local temperature, corresponding to the Tolman temperature [52],  $T = (g_{00})^{-1/2}T_0$ , with  $T_0 = r_H/(2\pi\ell^2)$  being the Hawking temperature of the black hole. This suggests that the Wightman function is a thermal correlation function, indicating that the conformally coupled quantum field in black hole spacetime behaves as a heat bath at temperature  $T$ , with the corresponding vacuum state being the Hartle-Hawking vacuum [53].

For the static detector outside the horizon, the transition rate is given by [30]:

$$\Gamma(\Omega) = \frac{1}{2} \left( \frac{1}{e^{\Omega/T} + 1} \right) \sum_{n=-\infty}^{+\infty} \left( P_{-\frac{1}{2}+i\frac{\Omega}{2\pi T}}(\cosh \alpha_n^-) - \zeta P_{-\frac{1}{2}+i\frac{\Omega}{2\pi T}}(\cosh \alpha_n^+) \right), \quad (18)$$

where  $P_\nu(x)$  is the associated Legendre function of the first kind [54], and

$$\begin{aligned} \cosh \alpha_n^\mp &= \frac{r_H^2}{r^2 - r_H^2} \left[ \frac{r^2}{r_h^2} \cosh\left(\frac{r_H}{\ell} 2\pi n\right) \mp 1 \right] \\ &= (1 + 4\pi^2\ell^2 T^2) \cosh\left(2\pi n\sqrt{M}\right) \mp 4\pi^2\ell^2 T^2. \end{aligned} \quad (19)$$

The  $n = 0$  term is independent of the mass parameter and corresponds to the transition rate of a uniformly accelerating detector in anti-de Sitter space. The  $n \neq 0$  terms represent genuine black hole contributions, with their effects being most significant for small  $M$  [55]. Besides, the Lamb shift of the detector, resulting from its interaction with the conformal field, has been analyzed in [56]. The Legendre functions satisfy the relation  $P_{-\frac{1}{2}+i\xi}(x) = P_{-\frac{1}{2}-i\xi}(x)$ , from which it follows that for all boundary conditions the transition rate is thermal, i.e., it satisfies the detailed balance condition

$$\Gamma(\Omega) = e^{-\beta\Omega}\Gamma(-\Omega). \quad (20)$$

As a result, in the long-time asymptotic limit, the detector reaches a thermal equilibrium state [44],

$$\rho_\infty = \frac{1}{2} \begin{pmatrix} 1 - \tanh(\beta\Omega/2) & 0 \\ 0 & 1 + \tanh(\beta\Omega/2) \end{pmatrix}, \quad (21)$$

at the KMS temperature  $T$ . Hereafter, we measure temperature  $T$  and energy  $\Omega$  in units of  $\ell^{-1}$  by setting  $\ell = 1$ , and time  $\tau$  in units of  $\lambda^{-2}$  by setting  $\lambda = 1$ . We remark that while the detector's transition rate, given by Eq. (18), strongly depends on the type of boundary conditions—Neumann, transparent, or Dirichlet—satisfied by the field in the BTZ spacetime (see, Fig. 1, and the relevant analysis in [55]), its asymptotic state remains unique, regardless of these conditions. This highlights the importance of considering the finite-time dynamics

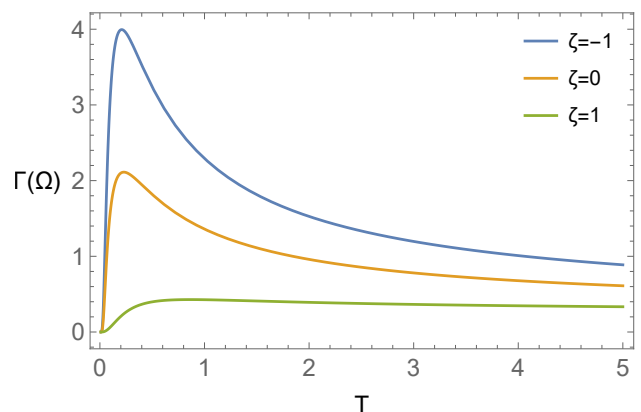


FIG. 1: The transition rate, Eq. (18), of a static UDW detector interacting with a conformally coupled field in a (2+1)-BTZ black hole background, as a function of the KMS temperature  $T$ , for the three boundary conditions satisfied by the field at spatial infinity. Here,  $M = 0.01$ , and  $\Omega = 0.1$ .

of a relativistic quantum Otto thermal machine within the open-system framework described in Sec. II A as the choice of boundary conditions significantly affects the machine output power.

#### IV. QUANTUM OTTO MACHINES IN BTZ SPACETIME

Now we utilize the thermal properties of the conformal field in the BTZ black hole background to model the field as a heat reservoir, with the UDW detector as the working medium, and investigate the performance of a relativistic quantum Otto machine. To investigate the thermodynamic properties of the Otto cycle, we define respectively the changes in heat and work [57],

$$\langle Q \rangle = \int_0^\tau dt \operatorname{tr} \left( \dot{\rho}(t) H(t) \right), \quad (22)$$

$$\langle W \rangle = \int_0^\tau dt \operatorname{tr} \left( \rho(t) \dot{H}(t) \right), \quad (23)$$

for a quantum system with density matrix  $\rho(t)$  evolving under a time-dependent Hamiltonian  $H(t)$ , and interacting with an external environment. Then, the first law of thermodynamics reads

$$\Delta U = \int_0^\tau dt \frac{d}{dt} \operatorname{tr} \left( \rho(t) H(t) \right) = \langle Q \rangle + \langle W \rangle, \quad (24)$$

where  $\Delta U$  is the change in the internal energy of the system. We start with the initial state of the working medium, a qubit detector, prepared with an energy gap  $\Omega_c$  between its two energy levels as follows,

$$\rho_{in} = \frac{1}{2} \begin{pmatrix} 1 - \tanh(\beta_c \Omega_c / 2) & 0 \\ 0 & 1 + \tanh(\beta_c \Omega_c / 2) \end{pmatrix}. \quad (25)$$

The quantum Otto thermodynamic cycle comprises four consecutive strokes, as described below:

(1.) Adiabatic expansion – The working medium undergoes an adiabatic expansion, during which its energy gap increases from  $\Omega_c$  to  $\Omega_h$ , with  $\Omega_h > \Omega_c$ , while it remains isolated from the field environment. The qubit remains in the initial state  $\rho_{in}$  and there is no heat exchange during the process. Thus, the change in the system internal energy is identified as work, given by

$$\langle W_1 \rangle = \frac{\Omega_h - \Omega_c}{2} \operatorname{tr} (\rho_{in} \sigma_3), \quad (26)$$

where  $\operatorname{tr} (\rho_{in} \sigma_3) = -\tanh(\beta_c \Omega_c / 2)$ .

(2.) Hot isochore – The working medium, with free Hamiltonian  $H_0 = \Omega_h \sigma_3 / 2$ , is coupled to a conformally coupled quantum field in the BTZ black hole spacetime, at the inverse KMS temperature  $\beta_h^{-1}$ , as given by Eq. (17), with  $\beta_h^{-1} > \beta_c^{-1}$ . Due to the interaction with the field, the populations of the energy levels of the system

change and its density matrix evolves from  $\rho_{in}$  to  $\rho_h(\tau_h)$ . The system dynamics is described by the second-order master equation, Eq. (7). The mean heat exchanged with the field during the process is

$$\langle Q_h \rangle = \frac{\Omega_h}{2} \operatorname{tr} [(\rho_h(\tau_h) - \rho_{in}) \sigma_3], \quad (27)$$

where

$$\begin{aligned} \operatorname{tr} (\rho_h(\tau_h) \sigma_3) &= -e^{-\gamma_h \tau_h} \tanh(\beta_c \Omega_c / 2) \\ &\quad - (1 - e^{-\gamma_h \tau_h}) \tanh(\beta_h \Omega_h / 2). \end{aligned} \quad (28)$$

(3.) Adiabatic compression – The working medium is isolated from the field environment and undergoes an adiabatic contraction, during which its energy gap decreases back to its initial value  $\Omega_c$ . The mean work done during this step is

$$\langle W_3 \rangle = \frac{\Omega_c - \Omega_h}{2} \operatorname{tr} (\rho_h(\tau_h) \sigma_3). \quad (29)$$

(4.) Cold isochore – The working medium interacts with a conformally coupled quantum field in the BTZ background spacetime at temperature  $\beta_c^{-1}$ . The population of the system energy levels change as a result of the interaction, and its state evolves as  $\rho_c(\tau_c)$ . The mean heat transferred during the process reads

$$\langle Q_c \rangle = \frac{\Omega_c}{2} \operatorname{tr} [(\rho_c(\tau_c) - \rho_h(\tau_h)) \sigma_3], \quad (30)$$

where

$$\begin{aligned} \operatorname{tr} (\rho_c(\tau_c) \sigma_3) &= e^{-\gamma_c \tau_c} \operatorname{tr} (\rho_h(\tau_h) \sigma_3) \\ &\quad - (1 - e^{-\gamma_c \tau_c}) \tanh(\beta_c \Omega_c / 2). \end{aligned} \quad (31)$$

At the end of the cycle, the working medium should be back to its initial state, to obtain a closed thermodynamic cycle (that is,  $\rho_c(\tau_c) = \rho_{in}$ ). This is satisfied in the long-time limits,  $\gamma_h \tau_h \gg 1$ , and  $\gamma_c \tau_c \gg 1$ , during steps (2) and (4) of the cycle, when the detector reaches its asymptotic equilibrium state. In this asymptotic regime, the heat and work changes read

$$\begin{aligned} \langle Q_h \rangle &= \frac{\Omega_h}{2} \left( \tanh(\beta_c \Omega_c / 2) - \tanh(\beta_h \Omega_h / 2) \right), \\ \langle W_3 \rangle &= \frac{\Omega_h - \Omega_c}{2} \tanh(\beta_h \Omega_h / 2), \\ \langle Q_c \rangle &= \frac{\Omega_c}{2} \left( \tanh(\beta_h \Omega_h / 2) - \tanh(\beta_c \Omega_c / 2) \right). \end{aligned} \quad (32)$$

#### A. Quantum Otto heat engine

In this case, heat is absorbed from the hot environment,  $\langle Q_h \rangle \geq 0$ , and flows into the cold  $\langle Q_c \rangle \leq 0$ . The work is extracted from the working medium for positive total work  $W = -(\langle W_1 \rangle + \langle W_3 \rangle) > 0$ . This implies the condition  $\Omega_h / \Omega_c < T_h / T_c$ . The efficiency  $\eta$  of a quantum

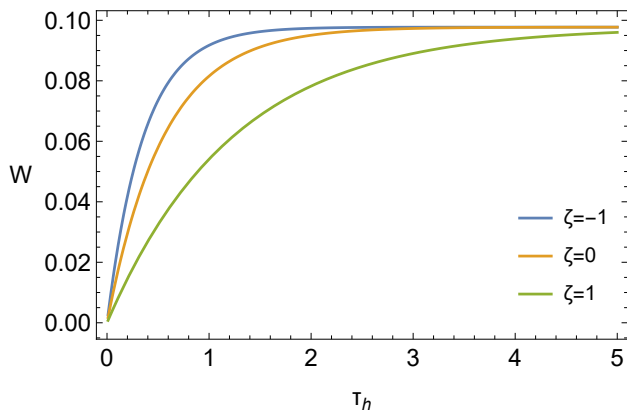


FIG. 2: Total work output of the heat engine as a function of the evolution time  $\tau_h$ , for the Neumann ( $\zeta = -1$ ), transparent ( $\zeta = 0$ ) and Dirichlet ( $\zeta = 1$ ) boundary conditions, satisfied by the conformally coupled field at spatial infinity. The parameters used for the plot are  $M = 0.01$ ,  $\Omega_h = 1$ ,  $\Omega_c = 0.1$ ,  $T_h = 2$ ,  $T_c = 0.1$ .

Otto heat engine is defined as the ratio of the total work output to the absorbed heat, then reads

$$\eta = -\frac{\langle W_1 \rangle + \langle W_3 \rangle}{\langle Q_h \rangle} = 1 - \frac{\Omega_c}{\Omega_h}, \quad (33)$$

and the power output as the total work to the duration  $\tau_{\text{cycle}}$  of the cycle,

$$P = -\frac{\langle W \rangle_{\text{tot}}}{\tau_{\text{cycle}}}. \quad (34)$$

Without loss of generality, we explicitly account for the durations of the heating and cooling strokes, writing  $\tau_{\text{cycle}} = \tau_h + \tau_c$ , while neglecting the duration of the adiabatic strokes.

In Fig. 2, we plot the total work done by the qubit detector as a function of the evolution time  $\tau_h$  (in units of  $\lambda^{-2}$ ) for the three different boundary conditions satisfied by the conformally coupled scalar field in the BTZ space-time. We observe that the total work reaches its maximum output in the long-time limit, asymptotically approaching the values given in Eqs. (32), which are independent of the boundary conditions. However, for finite engine operation times  $\tau_h$ , the work output strongly depends on the boundary conditions. At earlier times, the Neumann boundary condition ( $\zeta = -1$ ) yields the highest work output. This case also surpasses the other two boundary conditions in reaching the maximum asymptotic value in earlier times.

The maximum efficiency of a heat engine is determined by the Carnot efficiency [9], given by  $\eta_C = (T_h - T_c)/T_h$ . However, reaching Carnot efficiency requires an infinite slow process to ensure perfect adiabatic evolution and complete thermalization with the heat reservoirs during each of the four strokes of the cycle, resulting in zero power output. A more practical measure for analyzing

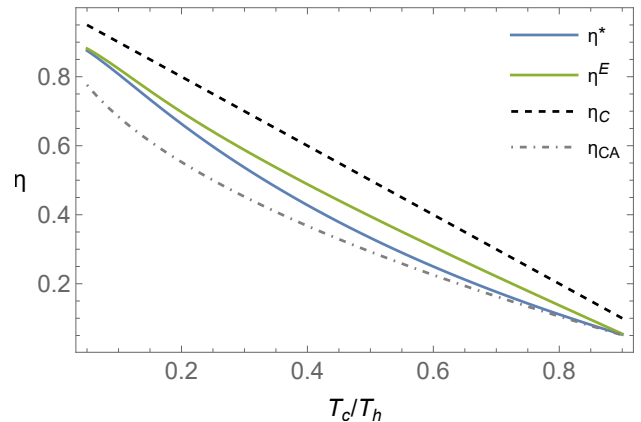


FIG. 3: The efficiency of the relativistic Otto heat engine as a function of the temperature ratio  $T_c/T_h$ . Here,  $\eta^*$  is the engine's efficiency at maximum power, while  $\eta^E$  denotes the efficiency at maximum ecological function, both optimized with respect to the qubit's energy gap  $\Omega_h$ . Additionally,  $\eta_C$  is Carnot efficiency, and  $\eta_{CA}$  the Curzon-Ahlborn efficiency. The parameters used for the plots are:  $M = 0.01$ ,  $\zeta = -1$ ,  $\Omega_c = 0.1$ ,  $\tau_h = 0.2$ ,  $\tau_c = 0.5$ .

the performance of a heat engine is the *efficiency at maximum power* (EMP), which is determined by first optimizing the power output with respect to a system parameter and then calculating the efficiency at that optimized power. Curzon and Ahlborn [10] derived the efficiency of a Carnot engine operating at maximum power as  $\eta_{CA} = 1 - \sqrt{T_c/T_h}$ . It balances the trade-off between high power output and low entropy production, incorporating the environmental impact of heat engines.

The *ecological criterion*, introduced by Angulo-Brown [41], is an alternative optimization criterion for evaluating the performance of heat engines. It embodies a compromise between maximizing useful work and minimizing the environmental cost of waste heat and entropy production. This criterion is implemented using the ecological function:

$$E = P - T_c S, \quad (35)$$

where  $S$  is total entropy change per unit time of the cycle, given by  $S = \beta_c \langle Q_c \rangle - \beta_h \langle Q_h \rangle$ .

We analyze the performance of the relativistic Otto heat engine, optimizing both the power output, Eq. (34), and the ecological function, Eq. (35), with respect to the energy gap  $\Omega_h$  of the qubit detector. The optimization is performed for fixed values of the parameters  $M$ ,  $\zeta$ ,  $T_h$ ,  $\Omega_c$ ,  $\tau_h$  and  $\tau_c$ , by numerically solving equations  $\partial P/\partial \omega_h = 0$  and  $\partial E/\partial \omega_h = 0$ . We then evaluate the efficiency at maximum power  $\eta^*$ , and at maximum ecological function  $\eta^E$ . In Fig. 3, we present the performance of the heat engine as a function of the temperature ratio  $T_c/T_h$ .

We verify numerically that the efficiency at maximum power coincides for the three different boundary conditions. As a result, we conclude that the Neumann bound-

ary condition represents the optimal case, as it yields the highest power output for finite-time operation of the heat engine. The EMP also exceeds the Curzon-Ahlborn  $\eta_{CA}$  in the intermediate temperature ratio range, which is similar to the result of the BTZ black hole Brayton engine cycle [39]. In addition, we observe that in the intermediate temperature ratio range the efficiency at the maximum ecological function  $\eta^E$  is different to the EMP  $\eta^*$ . When the ecological function is maximum, the heat engine releases a small amount of heat to the surrounding environment, making its operation more ecological. We remark that both the finite-time EMP values  $\eta^E$  and  $\eta^*$  closely resemble the ones analytically obtained in [58] for a qubit heat engine in the high-temperature regime, and converge to the same values in the long-time asymptotic limit.

### B. Quantum Otto refrigerator

The Otto thermodynamic cycle operates as a refrigerator when heat is absorbed from the cold environment,  $\langle Q_c \rangle \geq 0$ , and flows into the hot environment,  $\langle Q_h \rangle \leq 0$ . That is, satisfying the condition  $\Omega_h/\Omega_c > T_h/T_c$ .

In Fig. 4, we plot the cooling power  $\langle Q_c \rangle$ , as a function of the evolution time  $\tau_c$  for Neumann, transparent and Dirichlet boundary conditions. We confirm numerically that the absorbed heat reaches its maximum value in the long-time limit, asymptotically approaching the values given in Eq. (32). We observe that, for the Dirichlet boundary condition, and for fixed  $\tau_h$ , achieving this asymptotic value requires significantly longer times  $\tau_c$  than the other two cases. This results from the lower transition probabilities between the detector's energy levels in the low-temperature regime, as shown in Fig. (1). Similarly to the heat engine scenario, for finite-time operation of the refrigerator, the Neumann boundary condition again proves to be the optimal choice. It yields the highest cooling power and reaches the maximum asymptotic value much faster than the other two boundary conditions.

The *coefficient of performance* (COP)  $\varepsilon$  of an Otto refrigerator is defined as the ratio of heat absorbed from the cold environment to the total amount of work:

$$\varepsilon = \frac{\langle Q_c \rangle}{\langle W_1 \rangle + \langle W_3 \rangle} = \frac{\Omega_c}{\Omega_h - \Omega_c}, \quad (36)$$

where the second equality holds for a closed thermodynamic cycle. The maximum COP of a refrigerator is  $\varepsilon_C = T_c/(T_h - T_c)$  [9].

To optimize the performance of a refrigerator, we employ the *figure of merit*  $\chi$  [7], defined as the product of the COP and the cooling power  $\langle Q_c \rangle$  to the duration  $\tau_{cycle}$  of the cycle:

$$\chi = \frac{\varepsilon \langle Q_4 \rangle}{\tau_{cycle}}. \quad (37)$$

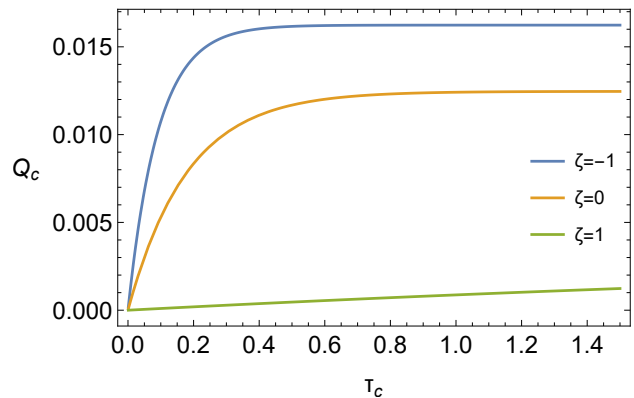


FIG. 4: Cooling power of the relativistic Otto refrigerator as a function of the evolution time  $\tau_c$  for the Neumann  $\zeta = -1$ , transparent ( $\zeta = 0$ ) and Dirichlet  $\zeta = 1$  boundary conditions. The parameters used for the plot are:  $M = 0.01$ ,  $\Omega_h = 0.5$ ,  $\Omega_c = 0.1$ ,  $T_h = 0.2$ ,  $T_c = 0.1$ ,  $\tau_h = 0.3$ .

On the other hand, the ecological criterion for refrigerators is implemented using the ecological function [58, 59]

$$E' = Q_c - \varepsilon_C T_h S. \quad (38)$$

We analyze the performance of the relativistic Otto refrigerator by optimizing the figure of merit, Eq. (37), and the ecological function, Eq. (38), with respect to the energy gap  $\Omega_c$  of the qubit detector. The optimization is performed for fixed values of the parameters  $M$ ,  $\zeta$ ,  $T_h$ ,  $\Omega_h$ ,  $\tau_h$  and  $\tau_c$ , by numerically solving equations  $\partial\chi/\partial\omega_c = 0$  and  $\partial E'/\partial\omega_c = 0$ . We now evaluate the COP at the maximum  $\chi$  figure of merit,  $\varepsilon^*$ , and the maximum ecological function,  $\varepsilon^E$ .

In Fig. 5, we present the COP of the refrigerator as a function of the temperature ratio  $T_c/T_h$ . We verify that the COP at maximum figure of merit coincides for the three different boundary conditions satisfied by the quantum field. Thus, we again conclude that the Neumann boundary condition represents the optimal case, and thus absorbs maximum heat from the cold field bath for finite-time operations. We observe that the COP at maximum ecological function  $\varepsilon^E$  is higher than the COP at maximum figure of merit  $\varepsilon^*$ , with both exceeding the Yan-Chen COP [60], which is the counterpart of the Curzon-Ahlborn efficiency for refrigerators, and is given by  $\varepsilon_{yan} = \sqrt{1 + \varepsilon_C} - 1$ . We note that both the finite-time COP values  $\varepsilon^*$  and  $\varepsilon^E$  closely resemble the ones that are analytically obtained in [58] for a qubit refrigerator in the high-temperature regime, and coincide in the long-time asymptotic limit.

## V. CONCLUDING REMARKS

We presented a general framework for studying the finite-time operation of relativistic quantum thermal machines, with a focus on their energy optimization. We applied this framework to study a UDW detector coupled

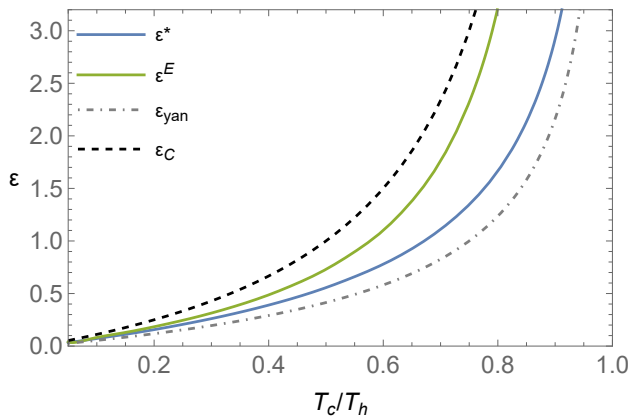


FIG. 5: Coefficient of performance (COP) of the relativistic Otto refrigerator as a function of the temperature ratio  $T_c/T_h$  (case  $\zeta = -1$ ). Here,  $\varepsilon^*$  is the COP at maximum figure of merit and  $\varepsilon^E$  the COP at maximum ecological function, both optimized with respect to the qubit's energy gap  $\Omega_c$ . Also,  $\varepsilon_C$  is the Carnot and  $\varepsilon_{yan}$  the Yan-Chen COP, respectively. The parameters used for the plot are:  $M = 0.01$ ,  $\Omega_h = 0.5$ ,  $\tau_h = \tau_c = 0.2$ .

to a quantum field in the Hartle-Hawking state in a BTZ black hole background spacetime, implementing an Otto

thermodynamic cycle with the detector as the working medium. By modeling the UDW detector as an open quantum system, with the field acting as a thermal bath, we described its finite-time dynamics in each stroke of the cycle. This approach allowed us to examine how the performance of an Otto heat engine or refrigerator is explicitly affected by Neumann, transparent, and Dirichlet boundary conditions imposed on the field. We identified the Neumann boundary condition as the optimal choice, yielding the highest work output and cooling power.

Since achieving Carnot efficiency represents an idealized case requiring perfect adiabatic evolution and complete thermalization at each stage of the thermodynamic cycle, we focused on optimizing the Otto thermal machine's performance in terms of power and ecological impact. This approach can be directly applied to detectors following different stationary trajectories in various curved spacetime backgrounds. Thus, our work provides a comprehensive analysis of quantum thermal machines and their energy optimization in relativistic settings.

## VI. ACKNOWLEDGMENTS

This work was supported by the UK Research and Innovation Engineering and Physical Sciences Research Council [grant number EP/Z002796/1].

- 
- [1] S. Vinjanampathy and J. Anders, Quantum thermodynamics, *Contemporary Physics* **57**, 545 (2016).
  - [2] F. Binder, L. Correa, C. Gogolin, J. Anders, and G. Adesso, *Thermodynamics in the Quantum Regime: Fundamental Aspects and New Directions*, Fundamental Theories of Physics (Springer International Publishing, 2018).
  - [3] S. Deffner and S. Campbell, *Quantum Thermodynamics*, 2053-2571 (Morgan & Claypool Publishers, 2019).
  - [4] P. P. Potts, *Quantum thermodynamics* (2024), arXiv:2406.19206 [quant-ph].
  - [5] N. M. Myers, O. Abah, and S. Deffner, Quantum thermodynamic devices: From theoretical proposals to experimental reality, *AVS Quantum Science* **4**, 027101 (2022).
  - [6] O. Abah, J. Roßnagel, G. Jacob, S. Deffner, F. Schmidt-Kaler, K. Singer, and E. Lutz, Single-ion heat engine at maximum power, *Phys. Rev. Lett.* **109**, 203006 (2012).
  - [7] O. Abah and E. Lutz, Optimal performance of a quantum otto refrigerator, *Europhysics Letters* **113**, 60002 (2016).
  - [8] R. Kosloff and Y. Rezek, The quantum harmonic otto cycle, *Entropy* **19** (2017).
  - [9] H. B. Callen, *Thermodynamics and an introduction to thermostatistics* (Wiley, New York, NY, 1985).
  - [10] F. L. Curzon and B. Ahlborn, Efficiency of a carnot engine at maximum power output, *American Journal of Physics* **43**, 22 (1975).
  - [11] S. Deffner, Efficiency of harmonic quantum otto engines at maximal power, *Entropy* **20** (2018).
  - [12] N. D. Birrell and P. C. W. Davies, *Quantum Fields in Curved Space*, Cambridge Monographs on Mathematical Physics (Cambridge University Press, 1982).
  - [13] S. W. Hawking, Particle Creation by Black Holes, *Commun. Math. Phys.* **43**, 199 (1975).
  - [14] W. G. Unruh, Notes on black-hole evaporation, *Phys. Rev. D* **14**, 870 (1976).
  - [15] B. S. DeWitt, Quantum gravity: The new synthesis, in *General Relativity: an Einstein Centenary Survey*, edited by S. Hawking and W. Israel (Cambridge University Press, Cambridge, England, 1979).
  - [16] B. L. Hu, S.-Y. Lin, and J. Louko, Relativistic quantum information in detectors-field interactions, *Classical and Quantum Gravity* **29**, 224005 (2012).
  - [17] R. B. Mann and T. C. Ralph, Relativistic quantum information, *Classical and Quantum Gravity* **29**, 220301 (2012).
  - [18] E. Arias, T. R. de Oliveira, and M. Sarandy, The unruh quantum otto engine, *Journal of High Energy Physics* **2018**, 168 (2018).
  - [19] F. Gray and R. B. Mann, Scalar and fermionic unruh otto engines, *Journal of High Energy Physics* **2018**, 174 (2018).
  - [20] H. Xu and M.-H. Yung, Unruh quantum otto heat engine with level degeneracy, *Physics Letters B* **801**, 135201 (2020).
  - [21] G. R. Kane and B. R. Majhi, Entangled quantum unruh otto engine is more efficient, *Phys. Rev. D* **104**, L041701 (2021).
  - [22] D. Barman and B. R. Majhi, Constructing an entangled unruh otto engine and its efficiency, *Journal of High Energy Physics* **2022**, 46 (2022).

- [23] A. Mukherjee, S. Gangopadhyay, and A. S. Majumdar, Unruh quantum otto engine in the presence of a reflecting boundary, *Journal of High Energy Physics* **2022**, 105 (2022).
- [24] K. Gallock-Yoshimura, V. Thakur, and R. B. Mann, Quantum otto engine driven by quantum fields, *Frontiers in Physics* **11**, 1287860 (2023).
- [25] N. Papadatos, The quantum otto heat engine with a relativistically moving thermal bath, *International Journal of Theoretical Physics* **60**, 4210 (2021).
- [26] N. K. Kollas and D. Moustos, An exactly solvable relativistic quantum otto engine, *Phys. Rev. D* **109**, 065025 (2024).
- [27] K. Gallock-Yoshimura, Relativistic quantum otto engine: instant work extraction from a quantum field, *Journal of High Energy Physics* **2024**, 198 (2024).
- [28] M. Bañados, C. Teitelboim, and J. Zanelli, Black hole in three-dimensional spacetime, *Phys. Rev. Lett.* **69**, 1849 (1992).
- [29] M. Bañados, M. Henneaux, C. Teitelboim, and J. Zanelli, Geometry of the 2+1 black hole, *Phys. Rev. D* **48**, 1506 (1993).
- [30] G. Lifschytz and M. Ortiz, Scalar field quantization on the (2+1)-dimensional black hole background, *Phys. Rev. D* **49**, 1929 (1994).
- [31] S. Carlip, The (2 + 1)-dimensional black hole, *Classical and Quantum Gravity* **12**, 2853 (1995).
- [32] L. Hodgkinson and J. Louko, Static, stationary, and inertial unruh-dewitt detectors on the btz black hole, *Phys. Rev. D* **86**, 064031 (2012).
- [33] M. R. Preciado-Rivas, M. Naeem, R. B. Mann, and J. Louko, More excitement across the horizon, *Phys. Rev. D* **110**, 025002 (2024).
- [34] M. Spadafora, M. Naeem, M. R. Preciado-Rivas, R. B. Mann, and J. Louko, Deep in the knotted black hole, *Phys. Rev. D* **111**, 065013 (2025).
- [35] J. Foo, C. S. Arabaci, M. Zych, and R. B. Mann, Quantum signatures of black hole mass superpositions, *Phys. Rev. Lett.* **129**, 181301 (2022).
- [36] L. J. Henderson, R. A. Hennigar, R. B. Mann, A. R. Smith, and J. Zhang, Harvesting entanglement from the black hole vacuum, *Classical and Quantum Gravity* **35**, 21LT02 (2018).
- [37] K. Bueley, L. Huang, K. Gallock-Yoshimura, and R. B. Mann, Harvesting mutual information from btz black hole spacetime, *Phys. Rev. D* **106**, 025010 (2022).
- [38] Z. Tian, X. Liu, J. Wang, and J. Jing, Dissipative dynamics of an open quantum battery in the BTZ spacetime (2024), [arXiv:2409.09259 \[hep-th\]](https://arxiv.org/abs/2409.09259).
- [39] E. E. Ferketic and S. Deffner, Boosting thermodynamic performance by bending space-time, *Europhysics Letters* **141**, 19001 (2023).
- [40] H. P. Breuer and F. Petruccione, *The Theory of Open Quantum Systems* (Oxford University Press, New York, 2007).
- [41] F. Angulo-Brown, An ecological optimization criterion for finite-time heat engines, *Journal of Applied Physics* **69**, 7465 (1991).
- [42] F. Benatti and R. Floreanini, Entanglement generation in uniformly accelerating atoms: Reexamination of the unruh effect, *Phys. Rev. A* **70**, 012112 (2004).
- [43] D. Moustos and C. Anastopoulos, Non-markovian time evolution of an accelerated qubit, *Phys. Rev. D* **95**, 025020 (2017).
- [44] B. A. Juárez-Aubry and D. Moustos, Asymptotic states for stationary unruh-dewitt detectors, *Phys. Rev. D* **100**, 025018 (2019).
- [45] H. Yu and J. Zhang, Understanding hawking radiation in the framework of open quantum systems, *Phys. Rev. D* **77**, 024031 (2008).
- [46] G. Kaplaneck and C. P. Burgess, Hot accelerated qubits: decoherence, thermalization, secular growth and reliable late-time predictions, *Journal of High Energy Physics* **2020**, 8 (2020).
- [47] G. Kaplaneck and E. Tjoa, Effective master equations for two accelerated qubits, *Phys. Rev. A* **107**, 012208 (2023).
- [48] J. R. Letaw, Stationary world lines and the vacuum excitation of noninertial detectors, *Phys. Rev. D* **23**, 1709 (1981).
- [49] S. J. Avis, C. J. Isham, and D. Storey, Quantum field theory in anti-de sitter space-time, *Phys. Rev. D* **18**, 3565 (1978).
- [50] R. Kubo, Statistical-mechanical theory of irreversible processes. i. general theory and simple applications to magnetic and conduction problems, *Journal of the Physical Society of Japan* **12**, 570 (1957).
- [51] P. C. Martin and J. Schwinger, Theory of many-particle systems. i, *Phys. Rev.* **115**, 1342 (1959).
- [52] R. Tolman, *Relativity, Thermodynamics and Cosmology*, International series of monographs on physics (Clarendon Press, 1934).
- [53] J. B. Hartle and S. W. Hawking, Path-integral derivation of black-hole radiance, *Phys. Rev. D* **13**, 2188 (1976).
- [54] I. S. Gradshteyn and I. M. Ryzhik, *Table of integrals, series, and products* (Academic press, USA, 2014).
- [55] L. J. Henderson, R. A. Hennigar, R. B. Mann, A. R. Smith, and J. Zhang, Anti-hawking phenomena, *Physics Letters B* **809**, 135732 (2020).
- [56] Y. Yu, J. Zhang, and H. Yu, The lamb shift in the btz spacetime, *Journal of High Energy Physics* **2023**, 209 (2023).
- [57] R. Alicki, The quantum open system as a model of the heat engine, *Journal of Physics A: Mathematical and General* **12**, L103 (1979).
- [58] S. Singh and O. Abah, *Energy optimization of two-level quantum otto machines* (2020), [arXiv:2008.05002 \[cond-mat.stat-mech\]](https://arxiv.org/abs/2008.05002).
- [59] J. J. Fernández, Optimization of energy production in two-qubit heat engines using the ecological function, *Quantum Science and Technology* **7**, 035002 (2022).
- [60] Z. Yan and J. Chen, A class of irreversible carnot refrigeration cycles with a general heat transfer law, *Journal of Physics D: Applied Physics* **23**, 136 (1990).